Influence of the Polymer Charge Density on Lipid−Polyelectrolyte Complexes at the Air/Water Interface

K. de Meijere, G. Brezesinski,* T. Pfohl, and H. Möhwald

Max Planck Institute of Colloids and Interfaces, Am Muehlenberg 2, D-14476 Golm/Potsdam, Germany

Received: November 18, 1998; In Final Form: August 12, 1999

Coupling of a polyelectrolyte to a charged lipid monolayer changes the interplay between the lateral forces within the monolayer and the entropic forces in the polymer. This results in structure changes in the monolayer region. Charge dilution within the polymer can help to evaluate the role of electrostatic attraction. The structure of a negatively charged phosphatidic acid monolayer complexed with copolymers consisting of the positively charged diallyldimethylammoniumchloride and the neutral acrylamide in different ratios was studied by grazing incidence X-ray diffraction. Ellipsometry measurements were used to determine the thickness of the adsorption layers. Lipid−polyelectrolyte complexes exhibit rectangular lattices at low pressures. The tilt angles of the molecular chains relative to the surface normal decrease with decreasing charge of the polyelectrolyte. In a complex with 21% polymer charge, a transition to a hexagonal phase is observed at 35 mN/m. The oblique lattice of the DPPA monolayer on water is suppressed in all systems. The adsorption layer, consisting of ∼ 85% water, gets thicker with decreasing polymer charge. This is a result of the formation of loops and tails.

Introduction

Lipids are known for their ability to build a great variety of molecularly ordered phases, depending on the geometry of the molecules, the concentration, the molecular density, and the ionic conditions in the subphase.[1,2] Polyelectrolytes on the other hand are used in many industrial processes, such as sewage treatment and paper production.[3] The adsorption at interfaces often plays an important role.

For various applications, for example in filtration and separation technology, stable lamellar structures that are built of hydrophobic and hydrophilic regions are needed. A biomimetic approach to that problem is to design a lipid bilayer coupling to a polyelectrolyte.[4] An important question concerns the influence of the polymer binding on the membrane structure. Since the electrostatic attraction is the driving force in the adsorption process, the charge density is of great relevance for the complex formation.

The most simple model system for lipid−polyelectrolyte complexes is the monolayer at the air/water interface. This interface is of great interest for biochemical membrane problems as well as for technical applications where the ability for self-organization of a lipid in mono- or bilayers and the mechanical properties of a polymer can be combined.

Polyelectrolytes couple spontaneously to charged lipid monolayers at the air/water interface. In a specific example, the monolayer consists of a negatively charged phosphatidic acid (DPPA) to which a positively charged polyelectrolyte (PDADMAC) is electrostatically bound. It was found that the polyelectrolyte reduces the lateral lipid density, suppresses the oblique as well as the hexagonal structures of the monolayer on water, and increases the tilt angles of the molecular chains relative to the surface normal. PDADMAC couples as a rigid rod preferentially perpendicular to the chain tilt without forming any loops and tails.[5]

In the present paper the influence of charge density in a polymer on the structure of a monolayer on water as well as on the thickness of the adsorption layer is studied to answer the question on the role of different specific interactions within the system. The charge density of PDADMAC was varied by using copolymers of charged DADMAC and noncharged acrylamide (AA). The molecular structure of the monolayer was analyzed by grazing incidence X-ray diffraction. The thickness of the polymer layer could be estimated from ellipsometry measurements.

TABLE 1: Molecular Weights and Polydispersity Index M_w/M_n for the Different Copolymers

copolymer	M_w (g/mol)	M_w/M_n
CP-73	5.8×10^5	1.6
Cp-47	1.4×10^6	2.7
CP-21	4.0×10^6	7.4

Experimental Section

Materials. The enantiomeric lipid L-1,2-dipalmitoyl phosphatidic acid (DPPA) (purity 98%) was purchased from SIGMA (Taufkirchen, Germany) and spread from a 10^{-3} M solution in chloroform (Merck, Germany, p. a. grade) onto the polyelectrolytic subphase (10^{-3} M, referring to the molecular weight of one monomer unit). The copolymers with different charge densities were kindly synthesized by F. Brand (Fraunhofer-Institut für Angewandte Polymerforschung, Teltow, Germany) in a radical copolymerization.[6] The copolymers were available in three different compositions with 73% (CP-73), 47% (CP-47), and 21% (CP-21) of the charged DADMAC monomer. The molecular weights and the polydispersity index M_w/M_n, which is the molecular weight range in the sample, are given in Table 1. M_w is the weight-average molecular weight and M_n is the number-average molecular weight.

The polymers were dissolved in ultrapure water which was purified in a Millipore desktop filtering system leading to a specific resistance of 18.2 MΩcm.

10.1021/jp984470f CCC: $18.00
Published on Web 10/01/1999

The adsorption is a fast process and should be in equilibrium after only 5−10 min.[7] In the experiments described in this paper the polyelectrolyte was given 30 min to adsorb to be sure that equilibrium was reached.

Grazing Incidence X-ray Diffraction. The grazing incidence X-ray diffraction (GIXD) measurements were carried out on the liquid surface diffractometer at the undulator beamline BW1 at HASYLAB, DESY (Hamburg, Germany).[8,9] The monochromatic beam strikes the air/water interface in the sample cell at an angle of grazing incidence, which is below the critical angle of total external reflection. The diffracted intensity is detected by a linear position sensitive detector (PSD) (OED-100-M, Braun, Garching, Germany) as a function of the vertical scattering angle α_f. Scanning the horizontal angle $2\theta_{xy}$, the horizontal and the vertical components of the scattering vector **Q** can be detected simultaneously. The in-plane divergence of the diffracted beam was restricted by a Soller collimator in front of the PSD to 0.09°. According to the diffraction geometry,[10] the horizontal (in-plane) component of the scattering vector Q_{xy} is given by $Q_{xy} \cong (4\pi/\lambda) \sin(2\theta_{xy}/2)$ and the vertical (out-of-plane) component by $Q_z \cong (2\pi/\lambda) \sin(\alpha_f)$, where λ is the X-ray wavelength. Model peaks as products of a Lorentzian parallel and a Gaussian normal to the water surface were least-squares fitted to the diffraction peaks. The lattice parameters a, b, and γ, the unit cell area A_{xy} and the cross sectional area A_0 can be calculated from the in-plane maximum positions of the diffraction peaks, while the out-of-plane position is used to calculate the tilt angle t of the chains relative to the surface normal and the tilt azimuth.[11] The diffractometer is equipped with a film balance (R&K, Wiesbaden, Germany) which carries a Wilhelmy-type system to record the lateral pressure π as a function of the molecular area. The same kind of film balance was used to measure pressure/area isotherms.

The ellipsometric measurements were performed on a picometer ellipsometer from Beaglehole instruments (Wellington, New Zealand) with a time resolution better than 20 ms and a beam area of about 1 mm^2. The phase modulated beam hits the water surface at the Brewster angle of $\Phi_B = 53.1°$. The imaginary part of the measured reflectivities $\mathrm{Im} = r_p/r_s$, where r_p and r_s are the amplitudes of p- and s-polarized waves, equals the ellipticity $\bar{\rho}$, if the real part Re of the reflectivity coefficient is zero. The difference between the pure water and the film covered surface is $\Delta\bar{\rho}$.[12]

$\Delta\bar{\rho}$ is related to the dielectric constants ϵ_1 and ϵ_2 of two adjacent bulk phases and to the dieletric constant ϵ_z along the surface normal (Drude model). For thin films at the air/water interface $\Delta\bar{\rho}$ is proportional to the film thickness d. The adsorption of a polyelectrolyte underneath a lipid monolayer can be detected as an increase of the ellipticity, which means an increase of d.[13] For thicker films (> 100 Å, where $\mathrm{Re}(r) > 0$), the complete Fresnel equations have to be used to calculate the film thickness and the refractive index.[14] The ellipticity of a multilayer system of a lipid monolayer and a thin polyelectrolyte adsorption layer can be taken as the sum of the ellipticities of these two single layers.

Results

Figure 1 shows the π/A isotherms of a DPPA monolayer after the adsorption of three partly charged copolymers compared to the isotherm of DPPA coupled to the fully charged polyelectrolyte PDADMAC at $T = 20$ °C. Especially at lower pressures the isotherms are shifted toward larger areas per molecule. This shift increases with decreasing polymer charge. The slope of the pressure increase decreases if the polymer charge is reduced,

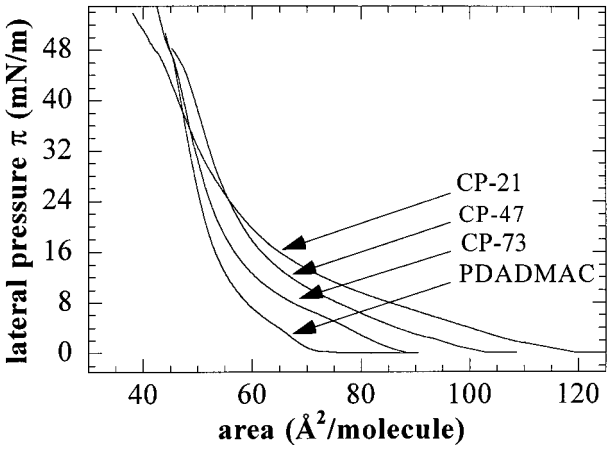

Figure 1. Pressure/area isotherms of DPPA monolayers coupled to polyelectrolytes with different charge densities at $T = 20$ °C.

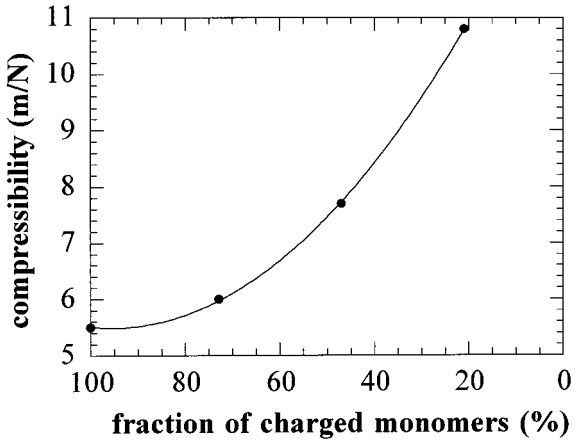

Figure 2. Mean lateral compressibilities at $\pi \geq 20$ mN/m for the coupled DPPA monolayer as a function of the polymer charge.

indicating an increase of the lateral compressibility κ, which is defined as

$$\kappa = -\frac{1}{A}\left(\frac{\partial A}{\partial \pi}\right)$$

The mean compressibilities for $\pi \geq 20$ mN/m for all DPPA/polyion complexes are shown in Figure 2. The increase is correlated to the increasing flexibility of the polymer as a result of a reduction of the electrostatic repulsion within the polymer. A greater flexibility of the polymer leads to a more flexible complex system.

X-ray diffraction measurements, carried out for the DPPA/CP-73 and the DPPA/CP-21 complexes, show a strong dependency of the molecular structure on the charge density in the polymer. The X-ray diffraction measurements of the coupled DPPA/CP-73 monolayer exhibit two diffraction peaks at all pressures investigated. Two contour plots that present the corrected X-ray intensities as a function of the in-plane component Q_{xy} and the out-of-plane component Q_z at $\pi = 20$ mN/m (a) and $\pi = 40$ mN/m (b) are shown in Figure 3. The two peaks observed indicate a rectangular lattice. Since they were found at $Q_z > 0$ Å^{-1} and $Q_z = 0$ Å^{-1} it can be concluded that the chains of the DPPA molecules are tilted toward their nearest neighbors (NN).[9]

In the contour plot of the DPPA/CP-21 monolayer at $\pi = 20$ mN/m (Figure 4a) one observes two maxima of a rectangular lattice with a tilt direction toward NN as well. After a phase transition only a single peak of a hexagonal lattice with untilted

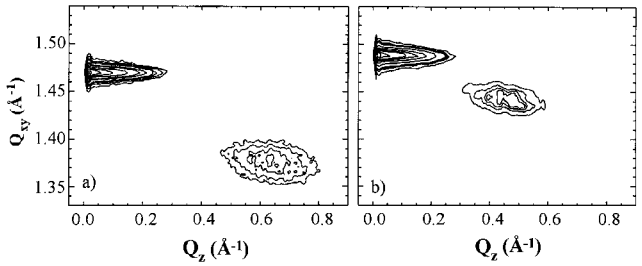

Figure 3. Contour plots of the corrected X-ray intensities as a function of the in-plane component Q_{xy} and the out-of-plane component Q_z of the scattering vector **Q** for a DPPA/CP-73 monolayer at $\pi = 20$ mN/m (a) and $\pi = 40$ mN/m (b).

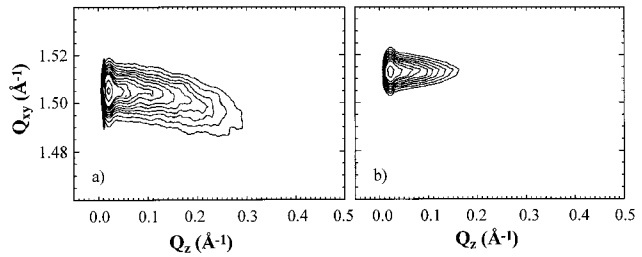

Figure 4. Contour plots of the corrected X-ray intensities as a function of the in-plane component Q_{xy} and the out-of-plane component Q_z of the scattering vector **Q** for a DPPA/CP-21 monolayer at $\pi = 20$ mN/m (a) and $\pi = 35$ mN/m (b).

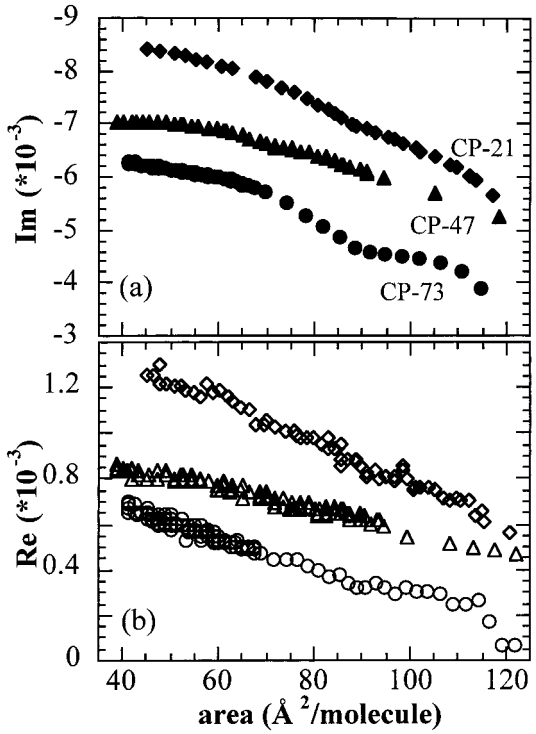

Figure 5. Imaginary (closed symbols) and real parts (open symbols) of the complex reflectivity coefficients as a function of the lateral pressure for DPPA/polyion monolayers with polyions of different charge densities (CP-73 (○,●); CP-47 (▲,△); CP-21 (◇,◆)).

chains could be found at $\pi = 35$ mN/m (Figure 4b). The peaks are found at larger values of Q_{xy} than those of the DPPA/CP-73 system at comparable pressures. Larger Q_{xy} values indicate smaller lattice spacings. The position of the 2-fold degenerate peak shifts to smaller Q_z values with increasing charge dilution in the polymer. This can be explained by a decrease of the tilt angles relative to the surface normal.

The ellipsometry measurements reveal the data presented in Figure 5. Since the imaginary part of the reflectivity coefficient is proportional to the film thickness, it can easily be concluded that the thickness of the adsorption layer increases with decreasing charge density of the polymer. For the polyelectrolytes CP-47 and CP-21 with lower charge densities, the values for the imaginary as well as for the real part of the reflectivity coefficient at large areas per molecule lie above the ones of the DPPA monolayer on pure water. They increase homogeneously with decreasing molecular area. The polymer already adsorbs in the coexistence region of the gaseous and a condensed phase. After the adsorption of CP-73 to the DPPA monolayer, the signal of the ellipsometer increases discontinuously at large molecular areas. This can be ascribed to heterogeneities due to the formation of domains of higher and lower ellipticity which are pushed together upon compression. Below an area of about 60−65 Å^2/molecule the thickness of the copolymer complex gets homogeneous just as it was observed for DPPA coupled to the fully charged PDADMAC. This effect corresponds to the beginning of the steep part of the isotherm.

Since the adsorption layers get thicker with decreasing charge density, the CP-21 system is thick enough to observe sufficiently large changes both in the real and the imaginary part to analyze the data using the complete Fresnel equations.[14] To estimate the thickness $d_{\text{CP-21}}$ of the adsorption layer and its refractive index $n_{\text{CP-21}}$, Im(CP-21) and Re(CP-21) are given by

$$\text{Im(CP-21)} = \text{Im(DPPA/CP-21)} - \text{Im(DPPA/H}_2\text{O)} = -0.0039$$

and

$$\text{Re(CP-21)} = \text{Re(DPPA/CP-21)} - \text{Re(DPPA/H}_2\text{O)} = 0.0007$$

Using the Fresnel equations, the thickness and the refractive index can be estimated to be

$$d_{\text{CP-21}} = 150 \pm 50 \text{ Å}$$

and

$$n_{\text{CP-21}} = 1.351 \pm 0.007$$

The relatively small changes in both parts of the measured reflectivity coefficients lead to large errors in the thickness determined.

To estimate the concentration of the polyelectrolyte at the interface and the water fraction in the adsorption layer, the refractive indices in the volume systems of all copolymers were determined with an ABBE refractometer. Since the increment $f(c) = dn/dc$ of the refractive index of polyelectrolytes is usually a constant value up to concentrations of about 0.4 g/mL, there is a linear relationship between the concentration of the polymer solution c_P and the refractive index n.[15] This linearity could be confirmed for the copolymers as it is shown in Figure 6. The increment and the refractive index are nearly independent of the charge density. This indicates that the composition of the polyelectrolyte has no measurable influence on the specific refractive index. Taking the refractive index of the CP-21 layer obtained from the ellipsometry measurements, the concentration of the polymer at the interface is $c_P \approx 0.15$ g/mL. Assuming a density of $\rho = 0.999$ g/mL[16] ≈ 1 g/mL, this concentration corresponds to a water content in the adsorption layer of ≈85% of the adsorbed amount of material. In a previous study[17] where the polyelectrolyte subphase contained 10^{-2} mol/l NaCl, it could be shown that the water content is independent of the charge density of the polymer. Assuming the same independence for

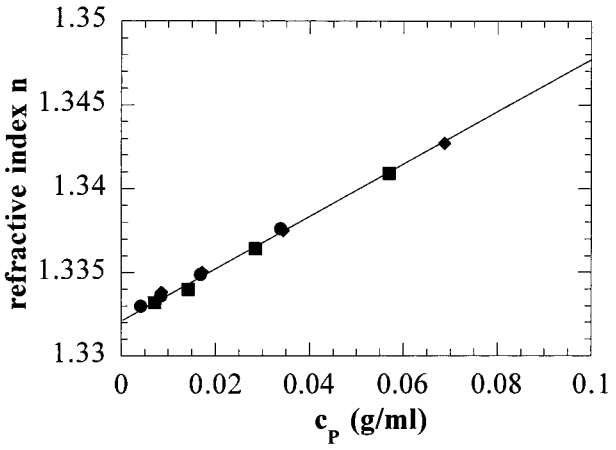

Figure 6. Refractive indices of the polyelectrolytes PDADMAC (▲), CP-73 (◆), CP-47 (■), and CP-21 (●) as a function of the polyelectrolyte concentration at $T = 20$ °C.

TABLE 2: Unit Cell Parameters *a*, *b*, and γ, Projected Area Per Chain A_{xy}, Cross-Sectional Area A_0, Tilt Angle *t*, and Positional Correlation Lengths $\xi_\perp$ and $\xi_{||}$ as Derived from the Analysis of the X-ray Diffraction Data of DPPA on CP-73 and on CP-21 at Different Surface Pressures π

π (mN/m)	*a* (Å)	*b* (Å)	γ (°)	*t* (°)	A_{xy} (Å^2)	A_0 (Å^2)	$\xi_\perp$ (Å)	$\xi_{||}$ (Å)
DPPA on CP-73								
3	5.63	5.13	123.3	33	24.1	20.4	44	206
10	5.59	5.12	123.1	32	23.9	20.4	50	224
20	5.42	5.06	122.4	29	23.1	20.3	52	265
30	5.27	5.00	121.8	25	22.4	20.3	54	265
40	5.06	4.92	120.9	19	21.3	20.2	56	265
DPPA on CP-21								
10	4.94	4.87	120.5	13	20.7	20.2	41	97
15	4.91	4.85	120.4	12	20.5	20.1	44	115
20	4.91	4.85	120.4	10	20.5	20.2	39	86
30	4.88	4.83	120.3	7	20.3	20.2	48	86
35	4.80	4.80	120.0	0	19.9			142

the salt-free system, the refractive indices are the same for all polyelectrolytes. Knowing the refractive index of CP-47 and CP-73, the thickness of the adsorption layers of these thinner systems can be estimated using the Drude model. Taking the measured ellipticities (equal to Im_{CP-47} and Im_{CP-73} for Re = 0) and $n_{CP-47} = n_{Cp-73} \approx 1.351$, the following thicknesses are obtained

$$d_{CP-47} = 90 \pm 15 \text{ Å}$$

and

$$d_{CP-73} = 75 \pm 10 \text{ Å}$$

The amount of adsorbed polymer increases with decreasing charge density. The polymer forms more loops and tails.

Discussion

The structure data derived from the X-ray diffraction measurements are presented in Table 2. Figure 7 presents the tilt angle as a function of the lateral pressure for DPPA monolayers complexed with CP-73 and CP-21. In addition, estimated boundaries between different phases are given by dashed vertical lines. The data of DPPA on pure water and DPPA coupled to the fully charged PDADMAC[5] are shown as a reference. The structure and the phase behavior of DPPA on CP-73 are qualitatively and quantitatively the same as on PDADMAC. The coupled system exhibits a rectangular lattice with a chain tilt toward the nearest neighbors (NN) at all pressures investigated.

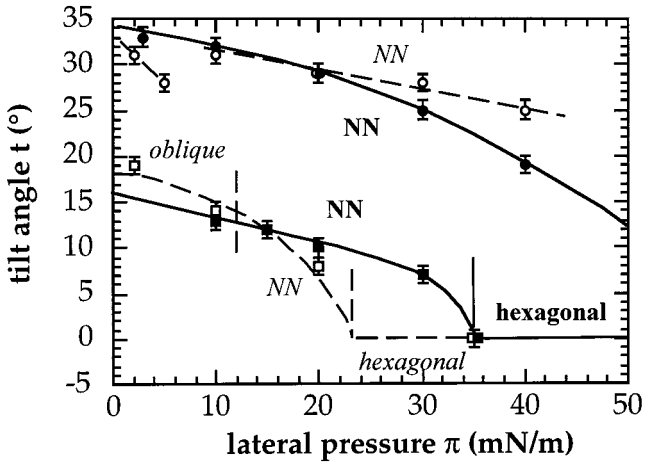

Figure 7. Schematic phase diagram: tilt angle *t* as a function of the lateral pressure π of a DPPA monolayer on water (□) and after the adsorption of PDADMAC (○), CP-73 (●), and CP-21 (■).

The tilt angles are largely increased compared to those of DPPA on water. At low pressure the tilt angles of the DPPA/CP-73 complex are nearly the same as for the DPPA/PDADMAC complex. The decrease of the tilt angles on increasing pressure is more pronounced for DPPA on CP-73 than on PDADMAC, indicating a slightly higher flexibility of the former system. The extrapolation of $1/\cos(t)$ plotted against the lateral pressure toward $t = 0°$ gives the transition pressure π_t to a phase with upright oriented chains.[18] This extrapolation leads to a π_t of 59 mN/m which is considerably lower than π_t for the DPPA/PDADMAC system of 92 mN/m. This phase transition could not be experimentally detected. The polyelectrolyte gets more flexible as a consequence of the charge dilution reducing the intramolecular electrostatic repulsion. Hence the charge distances and the adsorption points are not rigidly fixed. As a result the lateral van der Waals attraction leads to a denser packing, which is also reflected in the smaller area of the unit cell. At high pressure A_{xy} amounts to approximately 21 Å^2 compared to 22 Å^2 in the PDADMAC complex. The polyelectrolyte is still rigid enough to cause a lattice expansion compared to DPPA on water.

Decreasing charge density in the adsorption layer leads to further reduction of the tilt angles. Hence the chain tilt of the DPPA/CP-21 complex is decreased to values in the range of those for DPPA on pure water. The extrapolated transition pressure to the hexagonal phase is $\pi_t = 35$ mN/m and indeed a hexagonal lattice could be measured at 35 mN/m. At low and intermediate pressures the chains are ordered in a rectangular lattice with NN tilt.

The flexibility increases continuously with decreasing charge density. This increase can be correlated to the increasing compressibility which was determined from the isotherms. The molecular areas of DPPA/CP-21 at 35 mN/m are approximately 20 Å^2 per lipid chain. The lattice parameters are nearly the same as for DPPA on water. The influence of the weakly charged, very flexible CP-21 on the structure of the monolayer is significantly diminished. The lattice expansion is abolished. However, an oblique phase could also not be found in the DPPA/CP-21 film. The influence of chirality which leads to the formation of an oblique lattice of DPPA on pure water is suppressed because of the polyelectrolyte coupling.

A consequence of increasing flexibility is the formation of tails and loops in the adsorption layer which is the reason for the increasing thickness that could be observed in the ellipsometry measurements. Theoretical studies predict that the

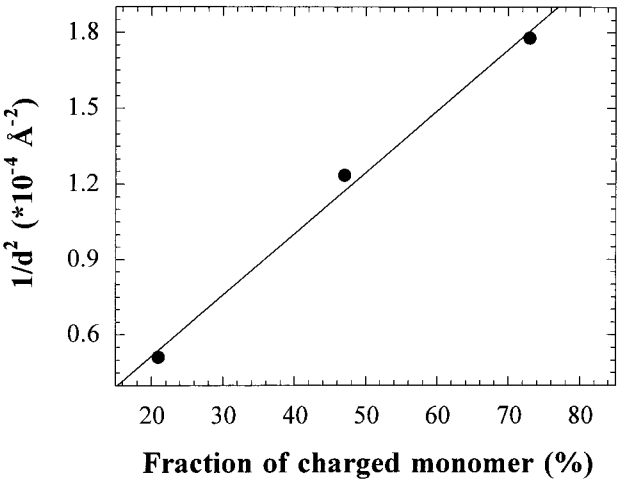

Figure 8. $1/d^2$ as a function of the charged monomer fraction in the polymer, with d as the thickness of the adsorption layer.

thickness of an adsorption layer of a strong polyelectrolyte in a solution of low ionic strength is proportional to the inverse square root of the charged polymer fraction.[19] Figure 8 shows a linear relationship between $1/d^2$, where d is the thickness of the adsorption layer, as a function of the charged fraction in the polymer. This linearity confirms the relationship predicted by theory.

A comparison of the molecular areas obtained from the isotherms and from the X-ray measurements shows a large discrepancy, especially at low pressure. This discrepancy can only be due to heterogeneities within the monolayer. The expansion can either be a result of uncoupled polymer segments penetrating between the lipid headgroups or of the formation of disordered lipid domains induced by the adsorption of polyelectrolyte. The penetration of polymer into the monolayer region is favored in low charge systems, since the fraction of the more hydrophobic acrylamide increases. Only those parts could possibly interact with the hydrophobic region of the monolayer. The heterogeneous composition of the monolayer could be confirmed by Brewster angle microscopy studies on the DPPA/CP-21 monolayer, revealing small domains of uniform diameter of about 25 μm. They appear much brighter than the rest of the monolayer indicating a larger thickness. The domains consist of ordered DPPA coupled to a thick layer of CP-21.

The full width at half-maximum of the in-plane diffraction peaks is related to the positional correlation lengths ξ in monolayers at the air/water interface.[5] The ξ values are generally larger perpendicular to the direction of the chain tilt ($\xi_\perp$) than parallel to it ($\xi_\parallel$). This phenomenon is due to one-dimensional crystallization in monolayers. In the DPPA/CP-73 film there is a conspicuous increase of the correlation perpendicular to the tilt and a decrease parallel to it compared to DPPA on pure water. The ratio perpendicular/parallel is 5:1. This is the same effect which was observed for DPPA on a PDADMAC subphase (ratio 6:1). In the latter system the effect was interpreted to be the result of a preferred adsorption direction of the polymer rod perpendicular to the chain tilt. Decreasing the polymer charge and increasing the flexibility, this preferential direction is slightly reduced for the CP-73 and abolished for the low charged CP-21. In the latter complex monolayer the ratio of about 2.5:1 is nearly the same as for DPPA on water. Comparing CP-73 with PDADMAC, the absolute values of the correlation lengths at an intermediate pressure of $\pi = 20$ mN/m show an increase. A little more flexibility within the polymer rod, and therefore a little less rigidity for the direction of the coupling, obviously helps to anneal defects and increase the positional correlation. If the polymer gets too flexible as in the case of the CP-21 and does not couple into a preferential direction the polymer induces disorder and decreases the correlation lengths.

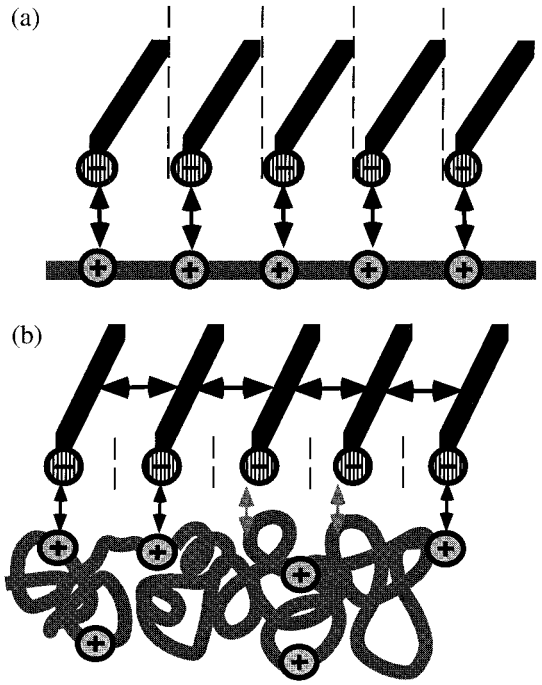

Figure 9. Schematic representation of the different interactions that are important for the formation of the monolayer structure for the DPPA/PDADMAC (top) and the DPPA/CP-21 system (bottom).

Conclusion

The interplay of interactions in the headgroup and the tail regions is one of the important factors for the structure formation in a lipid monolayer. Additional strong forces have to be taken into account if a polyelectrolyte electrostatically couples to the charged lipid monolayer. Comparing the fully charged PDADMAC with a partly charged copolymer allows to estimate the influence of the polymer charge density on the structure formation.

PDADMAC carries one positive charge per monomer unit and couples as a rigid rod in a 1:1 stoichiometry to a charged DPPA monolayer, preferentially perpendicular to the chain tilt of the lipid molecules. The electrostatic attraction (arrows) between the polymer and the lipid dominates the structure formation at all pressures (Figure 9, top). The fixed charge distances in the polyelectrolyte determine the distances of the molecules in the monolayer and the resulting structure. Neither the chiral interaction in the headgroup region nor the van der Waals attraction between the chains (dashed lines) can influence the structure formation dominated by the polymer coupling. Therefore, neither the formation of an oblique nor of a hexagonal packing is observed.

The adsorption of a partly charged copolymer to a DPPA monolayer shifts the sensitive equilibrium of the different interactions. The polyelectrolyte is more flexible and forms thicker adsorption layers with many loops and tails. The situation is schematically represented in Figure 9 (bottom) for a copolymer with a low charge density. The 1:1 stoichiometry might be eliminated as a result of the unfavorable relation between the charge densities. The adsorption might not only be a result of the electrostatic coupling (thin black arrows) but also of non

electrostatic contributions to the adsorption energy[20] (gray arrows). The adsorption layer is flexible enough to adapt to the packing constraints of the lipid molecules. The dominating force for the structure formation is the van der Waals interaction between the hydrophobic chains (thick black arrows). It causes a dense packing in a hexagonal lattice with perpendicularly oriented chains at high pressure. Despite a sufficient lattice expansion at low pressures, the fixed coupling points suppress the headgroup interactions (dashed lines) that lead to an oblique lattice in the DPPA monolayer on pure water.

Acknowledgment. We thank HASYLAB at DESY, Hamburg, for beam time and for providing all necessary facilities. H. Dautzenberg, MPI f. Kolloid- und Grenzflächenforschung, kindly donated the polymers. We thank the Deutsche Forschungsgemeinschaft (DFG) for financial support.

References and Notes

(1) Rosen, M. J. *Surfactants and Interfacial Phenomena*, 2nd ed.; John Wiley & Sons: New York, 1989.
(2) Gaines, G. L. *Insoluble Monolayers at the Liquid−Gas-Interface*; Interscience Publisher: New York, 1966.
(3) Mandel, M. *Polyelectrolytes*; Mandel, M., Ed.; John Wiley & Sons: New York, 1988; Vol. 11, p 739.
(4) Antonietti, M.; Kaul, A.; Thünemann, A. *Langmuir* **1995**, *11*, 2633.
(5) de Meijere, K.; Brezesinski, G.; Möhwald, H. *Macromolecules* **1997**, *30*, 2337.
(6) Brand, F.; Dautzenberg, H.; Jaeger, W.; Hahn, M. *Angew. Makromolek. Chemie* **1997**, *248*, 41.
(7) Sohling, U.; Schouten, A. F. *Langmuir* **1996**, *12*, 3912−3919.
(8) Als-Nielsen, J.; Jaquemain, D.; Kjaer, K.; Leveiller, F.; Lahav, M.; Leiserowitz, L. *Phys. Rep.* **1994**, *246*, 252.
(9) Kjaer, K. *Physica B* **1994**, *198*, 100−109.
(10) Kjaer, K. *Experimental Stations at HASYLAB*, Hasylab: Desy, 1994.
(11) Als-Nielsen, J.; Möhwald, H. In *Handbook of Synchrotron Radiation*; Ebashi, E. et al., Eds.; North-Holland: Amsterdam, 1991; Vol. 4.
(12) Beaglehole, D. *Physica B* **1980**, *100*, 163.
(13) Pfohl, T.; Riegler, H. *Phys. Rev. Lett.*, submitted for publication.
(14) Lekner, J.-A. *Theory of Reflection*; Martinus Nijhoff Publishers: Dordrecht, 1987.
(15) Feijter, J. A. D.; Benjamins, J.; Veer, F. A. *Biopolymer* **1978**, *17*, 1759.
(16) Brand, F. *Polyelektrolyte mit unterschiedlichen Ladungsdichten: Synthese, Charakterisierung, Polyelektrolyt-Komplexbildung*; Brand, F., Ed.; TU Berlin: Berlin, 1995.
(17) de Meijere, K.; Brezesinski, G.; Kjaer, K.; Möhwald, H. *Langmuir* **1998**, *14*, 4204.
(18) DeWolf, C.; Brezesinski, G.; Weidemann, G.; Möhwald, H.; Kjaer, K.; Howes, P. B. *J. Phys. Chem. B* **1998**, *102*, 3238−3242.
(19) Borukhov, I.; Andelman, D.; Orland, H. *Macromolecules* **1998**, *31*, 1665−1671.
(20) Stuart, M. A. C.; Fleer, G. J.; Lyklema, J.; Norde, W.; Scheutjens, J. M. H. M. *Adv. Colloid Interface Sci.* **1991**, *34*, 477−535.